Transient Two-dimensional Electronic Spectroscopy: Coherent Dynamics at Arbitrary Times along the Reaction Coordinate

Aritra Mandal, Jonathan D. Schultz, Yi-Lin Wu, Adam F. Coleman, Ryan M. Young* and Michael R. Wasielewski*

Department of Chemistry and Institute for Sustainability and Energy at Northwestern, Northwestern University, Evanston, IL 60208-3113, USA

E-mail: m-wasielewski@northwestern.edu; ryan.young@northwestern.edu

Abstract:

Recent advances in two-dimensional electronic spectroscopy (2DES) have enabled identification of fragile quantum coherences in condensed phase systems near the equilibrium molecular geometry. In general, traditional 2DES cannot measure such coherences associated with photophysical processes that occur at times significantly after the initially prepared state has dephased, such as the evolution of the initial excited state into a charge transfer state. We demonstrate the use of transient two-dimensional electronic spectroscopy (t-2DES) to probe coherences in an electron donor-acceptor dyad consisting of a perylenediimide (PDI) acceptor and a perylene (Per) donor. An actinic pump pulse prepares the lowest excited singlet state of PDI followed by formation of the $PDI^{\bullet-}$-$Per^{\bullet+}$ ion pair, which is probed at different times following the actinic pulse using 2DES. Analysis of the observed coherences provides information about electronic, vibronic, and vibrational interactions at any time along the reaction coordinate for ion pair formation.

TOC Graphic:

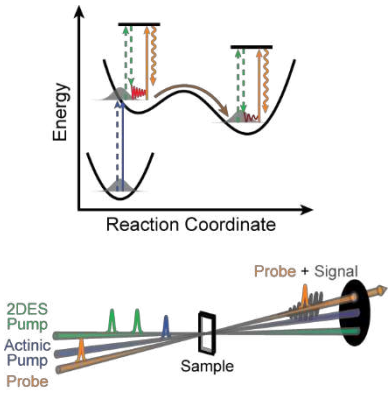

Quantum coherences between electronic or vibronic states are proposed to have profound effects on the function of many chemical, biological, and materials systems.[1-4] Recent advances in two-dimensional electronic spectroscopy (2DES) have enabled identification of these fragile quantum effects in disordered condensed-phase systems like photosynthetic antenna complexes,[1, 5-11] polymers[4, 12] and small molecules.[13-15] 2DES is a third-order nonlinear spectroscopic technique that uses three time-ordered ultrafast optical pulses:[16-17] the two initial light-matter interactions with two pump pulses can create coherences between two electronic or vibronic states near the equilibrium configuration of the system. These coherences appear as amplitude oscillations of different 2DES spectral features as a function of the waiting time (τ_2), which is the delay between the succeeding pump pulse and the probe pulse. Analysis of the origin and dephasing timescales of these coherent oscillations provides mechanistic insights into the roles of the molecular electronic and vibrational degrees of freedom in enabling efficient long-range energy transport in these systems immediately upon photoexcitation.

Such coherent effects and vibronic couplings are thought to have a strong influence on photoinduced charge transfer.[18-19] Photogeneration of the initial excited state of a donor-acceptor molecule is often followed by charge separation to varying degrees resulting in charge transfer (CT) or, in the limit, ion pair states. Charge separation is usually accompanied by significant nuclear reorganization in the molecules. Unfortunately, investigation of coherences in these CT or ion pair states cannot typically be achieved by conventional 2DES because it generates and measures coherences only near the Franck-Condon region of the initially prepared state. Moreover, in the excited-state manifold, conventional 2DES experiments can identify coherences between optically bright electronic/vibronic states only. However, in cases such as photoinduced charge transfer and singlet fission, for example, the relevant coherences are often associated with CT or

triplet states that are usually optically dark. While 2DES studies on such states have been performed,[15, 20-21] the necessary photophysical transformations must be extremely rapid and outcompete dephasing of coherences involving the dark states to be observed. In order to study electronic/vibronic coherences at any stage of a photoinduced process with no limitation on its timescale, here, we report transient two-dimensional electronic spectroscopy (t-2DES). Coherences launched and detected in these experiments at a given time delay from the initial photoexcitation can probe the interactions between electronic and/or vibrational degrees of freedom in states that are produced following preparation of the initial excited state.

The t-2DES experiments use an ultrafast optical excitation pulse, called an actinic pump, to populate the electronic state of interest followed by measuring the two-dimensional electronic spectra of the prepared state using the pulse sequence of conventional 2DES. The delay between the actinic pump and the first pulse of the 2DES pump pulse pair, τ_{act} (Figure 1A), can be varied to measure t-2DES spectra of the system at different stages of the photoinitiated process. Consequently, coherent oscillations from the t-2DES spectra can be obtained at different locations along the reaction coordinate (Figure 1B). Similar to traditional 2DES, coherences can be generated in t-2DES involving the state prepared by the actinic pump (analogous to the ground state in 2DES), or higher-lying states accessed via the 2DES pump. In this fashion, the actinic pump can also investigate coherences involving states that absorb deeper into the ultraviolet region which may be difficult in conventional 2DES.[22] It is also important to emphasize that the

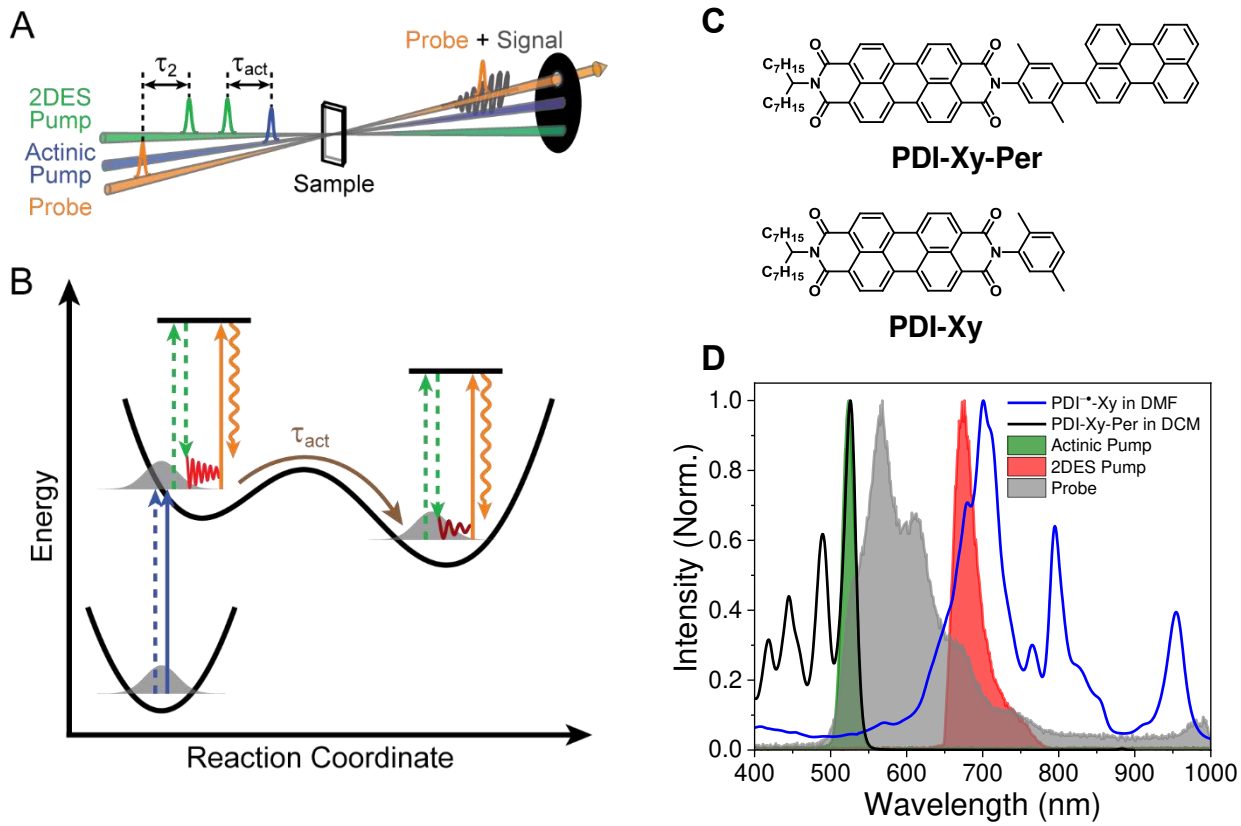

Figure 1. (A) Schematic representation of the beam geometry and pulse sequence used for the t-2DES experiments in this work. (B) Illustration of utilizing t-2DES to elucidate quantum coherences during different stages of a photophysical process. (C) Structures of PDI-Xy-Per and PDI-Xy. (D) Normalized linear UV-Vis absorption spectra of PDI-Xy-Per in DCM and of PDI$^{\bullet-}$-Xy in DMF, along with pulse spectra.

coherences interrogated by this technique are not necessarily the same as those that are potentially relevant from the initial photoexcitation event; they are induced at selected points along the reaction coordinate in order to probe the shape of the potential energy surface and to elucidate how the electronic/vibronic states may be interacting at a given time.

The implementation of t-2DES experiments has similarities to previously reported transient two-dimensional infrared spectroscopy (t-2DIR), except the latter uses ultrafast mid-IR pulses to measure the 2DIR spectra following electronic excitation of the molecules by an actinic pump pulse.[23-25] While the Raman-active modes investigated by t-2DES are resonance-enhanced, the

vibrational modes observed in t-2DIR are not. Therefore, t-2DES allows for direct interpretation of the influence of vibronic interactions along the reaction coordinate of a photophysical process. Additionally, the 2DES pump pulses that launch the Raman vibrational coherences in t-2DES have much broader bandwidths compared to narrowband Raman pump pulses used for the same purpose in femtosecond stimulated Raman spectroscopy (FSRS).[26-27] Consequently, information on vibronic coupling over a much broader spectral range is readily obtained in t-2DES. The precision with which the coherence is launched relative to populating the initial excited state determines the time resolution in t-2DES; this value is controlled by the cross-correlation between the actinic pump pulse and the first pulse of the 2DES pump pulse pair that launches the coherence.

Formally t-2DES is a fifth-order nonlinear spectroscopic technique and can be viewed as a two-dimensional extension of pump-degenerate four wave mixing spectroscopy.[28] However, the signal-to-noise of the detected coherences are improved in t-2DES as a result of dispersing the spectra along the pump frequency axis. Two-dimensional resonance Raman spectroscopy[29] as well as population-controlled impulsive Raman spectroscopy,[30-32] in comparison, do not disperse the spectra in the electronic excitation frequency. While pulse sequences similar to t-2DES have been used before in the context of coherent two-dimensional mass spectrometry,[33] the signal in t-2DES is detected coherently, as opposed to incoherent detection in the previous case. Other fifth-order nonlinear spectroscopic techniques like triggered-exchange 2DES cannot launch and measure coherences at an arbitrary time delay after initial photoexcitation,[34] nor can GAMERS, owing to the non-resonant interaction with the initial pump pulse.[35] Consequently, t-2DES offers more specific and detailed information on vibronic interactions. Furthermore, t-2DES can be extended to yield two-dimensional resonance Raman spectra by scanning and subsequent Fourier transform of τ_{act}.

As a proof-of-concept, we have utilized t-2DES spectroscopy to study a photoinduced charge transfer reaction within an electron donor-acceptor dyad comprising a perylene-3,4:9,10-bis-(dicarboximide) (PDI) acceptor and a perylene (Per) donor, separated by a xylene (Xy) spacer (PDI-Xy-Per, Figure 1C). The excited-state dynamics of PDI-Xy-Per are reasonably well-understood;[36] thus, it provides a useful platform for studying vibrational coherences from different states with similar electronic spectra using t-2DES. The actinic pump pulse was used to excite PDI-Xy-Per to ^{1*}PDI-Xy-Per, which undergoes charge transfer to generate PDI$^{\bullet-}$-Xy-Per$^{\bullet+}$.[36] Subsequently, by using 2DES pump pulses that are non-resonant with the ground-state absorption of PDI-Xy-Per but resonant with either ^{1*}PDI-Xy-Per or PDI$^{\bullet-}$-Xy-Per$^{\bullet+}$ transitions, we launch and measure coherences that occur long after the initial photoexcitation process.

For t-2DES experiments, we used 524 nm, 36 fs pulses as the actinic pump, and 17 fs pulses with a 648-780 nm spectrum for the 2DES pump (Figure 1D; see Figure S1 for temporal characterization). A broadband white-light continuum with a ~500-1000 nm spectrum was used as the probe pulse (Figure 1D). The experimental beam geometry for performing the t-2DES experiments is shown in Figure 1A. Similar to the pump-probe configuration for conventional 2DES measurements, the 2DES pump pulse pair propagate collinearly in t-2DES, after being generated by a pulse shaper.[37-38] The actinic pump pulse bisects the 2DES pump and probe pulses along the direction of propagation. The difference between two separate 2DES spectra, collected with and without the actinic pump, yields the t-2DES spectra. The signal with or without the actinic pump co-propagates with the probe pulse based on the phase matching condition and is detected by heterodyne mixing with the probe. In this experimental geometry, the measured t-2DES spectra are absorptive in nature. The formal fifth-order t-2DES signal depends on the relative polarization of the optical pulses.[39] While the polarizations of the 2DES pump and probe pulses were parallel

to each other for these experiments, they were perpendicular to that of the actinic pump pulse. Further details of the experimental setup and sample preparation are provided in the Supporting Information.

The linear absorption spectrum of PDI-Xy-Per in dichloromethane (DCM) exhibits several vibronic peaks (Figure 1D), with the 0–0 vibronic band of PDI centered at 526 nm. Excitation of this band has been shown to result in charge separation (CS) forming $PDI^{\bullet-}$-Xy-$Per^{\bullet+}$,[36] and therefore, the actinic pump (Figure 1D) initiates CS during the t-2DES measurements. In order to ascertain the spectral changes and timescales corresponding to the CS process, we performed conventional 2DES spectroscopy on PDI-Xy-Per using pump pulses centered at 524 nm and a white light pulse as the probe. The resultant 2DES spectra at a waiting time of 100 fs show overlapping ground-state bleach (GSB) and stimulated emission (SE) features centered at 532 nm together with a SE feature at 578 nm probe wavelengths (Figure S2).[40] The primary excited-state absorption (ESA) exhibits a maximum at a probe wavelength of 707 nm. At a waiting time of 40 ps, the 2DES spectrum exhibits photoinduced absorption (PIA) signals arising from the CT state with $PDI^{\bullet-}$ observed at 717 nm, 801 nm and 966 nm probe wavelengths, whereas $Per^{\bullet+}$ is observed at a 559 nm probe wavelength.[36] Evolution-associated spectral analysis on this 2DES dataset with a A → B → ground state (GS) model yields the time constants for charge separation and recombination as 6.22 ± 0.17 ps and 84.5 ± 2.3 ps, respectively, which are in good agreement with previously reported values.[36] The 2DES spectra of states A and B primarily show features of ^{1*}PDI-Xy-Per and $PDI^{\bullet-}$-Xy-$Per^{\bullet+}$, respectively (Figure S3).

With the population dynamics well understood, we performed t-2DES measurements at various τ_{act} to obtain two-dimensional electronic spectra at different stages of the charge separation process. Figure 2A shows representative t-2DES spectra of PDI-Xy-Per in DCM at varying τ_{act},

keeping τ_2 fixed at 500 fs (see Figure S5 for spectra at additional τ_{act}). Actinic pump delays of 1 ps, 6 ps and 40 ps are chosen to access different stages of the charge transfer process, as indicated by the arrows on the population kinetics obtained from the evolution-associated spectral analysis of the conventional 2DES data (Figure 2B).

There are three different types of signals that contribute to the t-2DES spectra: photoinduced bleach (PIB), photoinduced emission (PIE), and photoinduced absorption (PIA). Similar to the GSB, PIB signals result in negative absorption changes as population is removed from the transient state generated by the actinic pump. At τ_{act} = 1 ps, most of the population created by the actinic pump pulse remains in the excited electronic state, ^{1*}PDI-Xy-Per ($|S_1\rangle$). Consequently, the PIB features in the t-2DES spectra at τ_{act} = 1 ps appear at the same probe frequencies as the ESA features in the conventional 2DES measurements. The density matrix evolution corresponding to a representative pathway that results in the PIB signal at (λ_{pump}, λ_{probe}) = (698 nm, 707 nm) at τ_{act} = 1 ps is shown in Figure 2C (Pathway 1; others in Figure S7). In addition, there are two types of PIE signals obtained in t-2DES. One such signal, PIE-I, is observed at probe wavelengths near the steady-state emission peaks of PDI at 535 nm and 575 nm when τ_{act} = 1 ps.[40] A representative pathway contributing to the PIE-I signal at (λ_{pump}, λ_{probe}) = (698 nm, 535 nm) is also shown in Figure 2C (Pathway 2; others in Figure S7). PIE-I signals are produced only by pathways that do not involve population transfer during the waiting time and appear as positive changes in absorption in the t-2DES spectra. At τ_{act} = 40 ps, the population from the initially prepared excited state ^{1*}PDI-Xy-Per ($|S_1\rangle$) completely transfers to the CT state (PDI$^{\bullet-}$-Xy-Per$^{\bullet+}$, $|CT\rangle$). Thereafter, the interactions of the system with the 2DES pump and probe pulses result in diagonal and cross-peak PIB features at 717 nm, 801 nm and 966 nm probe wavelengths (pathways shown in Figure S7). These features appear at the same location as the PDI-centered absorption peaks of

PDI•⁻-Xy (Figure 1D).

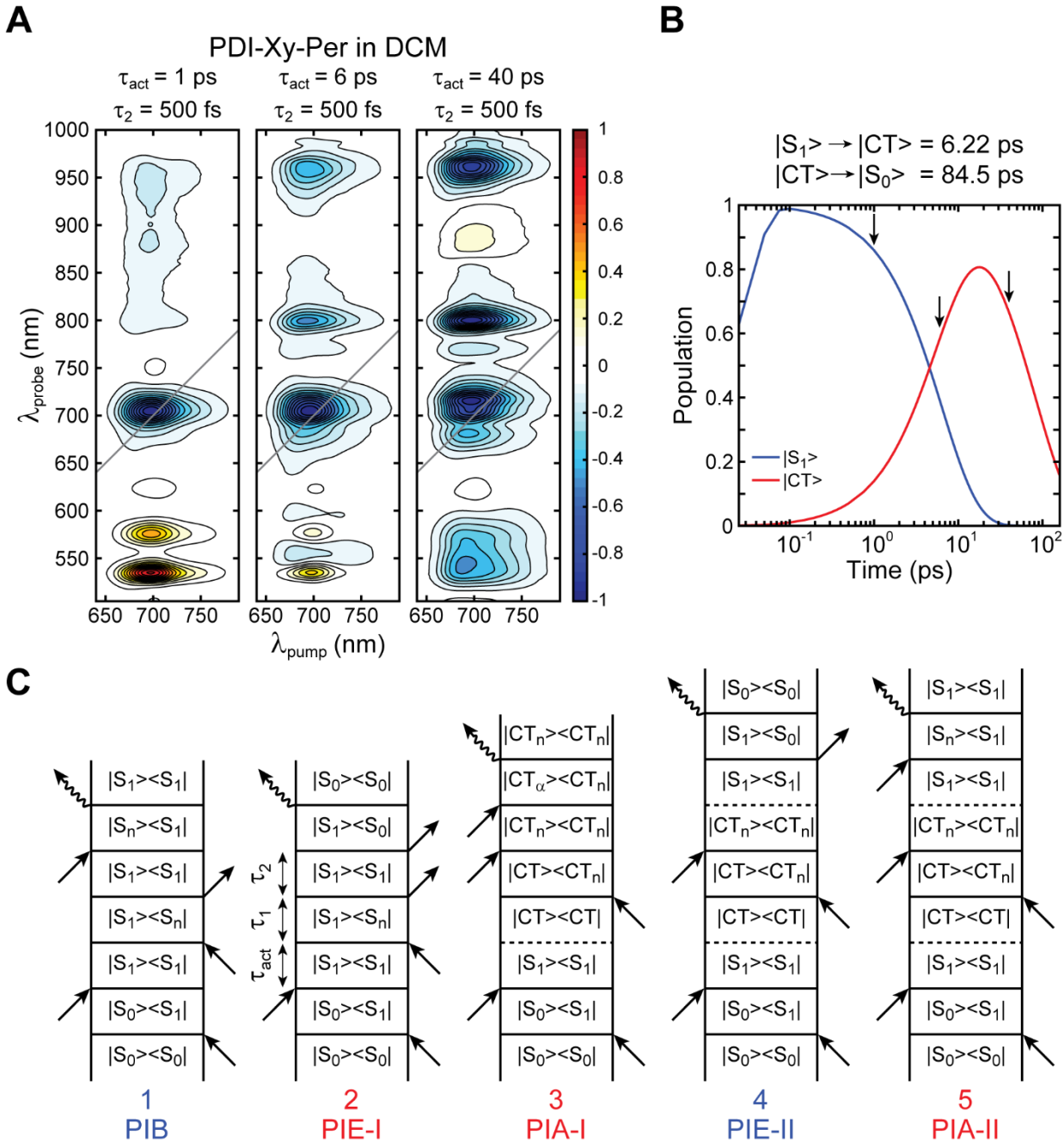

Figure 2. (A) t-2DES spectra of PDI-Xy-Per in DCM as a function of the actinic pump delay (τ_{act}). The spectra are normalized to the maximum absolute change in absorption at each (τ_{act}, τ_2). (B) Population evolution of different states obtained from the evolution-associated spectral analysis of conventional 2DES data on PDI-Xy-Per in DCM. The black arrows indicate the actinic delays used for measurement of t-2DES spectra. (C) Feynman diagrams corresponding to representative pathways resulting different types of t-2DES spectral features. The dotted horizontal lines indicate population transfer during the time period between two light-matter interactions.

Figure 3A shows representative t-2DES spectra at τ_{act} = 40 ps with varying τ_2 (see Figure S6 for spectra at additional τ_2). In addition to the PIB features observed in the t-2DES spectrum at (τ_{act}, τ_2) = (40 ps, 500 fs), the spectrum at (τ_{act}, τ_2) = (40 ps, 96 fs) exhibits a PIA feature, PIA-I, centered at 629 nm probe wavelength that arises from the $^{*}PDI^{\bullet-}$-Xy-$Per^{\bullet+}$ ($|CT_n\rangle$). Conventional 2DES measurements on chemically reduced PDI-Xy (Figure 1C) allow us to assign this feature (Figure S4). A representative pathway contributing to this signal is also shown in Figure 2C (Pathway 3; others in Figure S8). As a function of τ_2, this positive PIA-I signal disappears, and a negative PIE signal, PIE-II, appears with its center at 549 nm probe wavelength. The disappearance of the PIA-I signal is caused by charge recombination that transfers the population created by the 2DES pump in the excited CT state ($|CT_n\rangle$) back to the excited singlet state of the neutral molecule ^{1*}PDI-Xy-Per ($|S_1\rangle$) on ~375 fs timescale as determined by pump-pump-probe spectroscopy of PDI-Xy-Per (Figure S9). A representative pathway resulting this negative PIE-II signal is shown in Figure 2C (Pathway 4; others in Figure S8). In general, PIE-II signals in t-2DES spectra appear as negative signals and involve a unidirectional population transfer during the waiting time. As a result of charge recombination, a positive PIA signal, PIA-II, arising from the $|S_1\rangle$ state also appears. Even though this signal is mostly overshadowed by the stronger PIB signals from the $|CT\rangle$ state, a weak positive feature is observed at a 909 nm probe wavelength for longer waiting times at τ_{act} = 40 ps. A representative pathway for this PIA-II signal is shown in Figure 2C (Pathway 5; others in Figure S8).

In order to extract coherent oscillations from the 2DES or t-2DES, a series of spectra are collected at closely spaced waiting times (8 fs) up to τ_2 = 1 ps, yielding a frequency resolution of 33 cm^{-1} (see Supporting Information for details); then, the amplitude of the signal from a relevant spectral region is chosen and the population kinetics are subtracted from it.

The top panel of Figure 3B shows the power spectrum of the coherent oscillations obtained from the highlighted region of the PIB feature (Figure 3A center spectrum) of t-2DES spectra at an actinic pump delay of 40 ps. The peaks at 285 cm^{-1} and 703 cm^{-1} correspond to the Raman vibrational modes of DCM and are removed. The most notable $PDI^{\bullet-}$ vibrational modes appear at

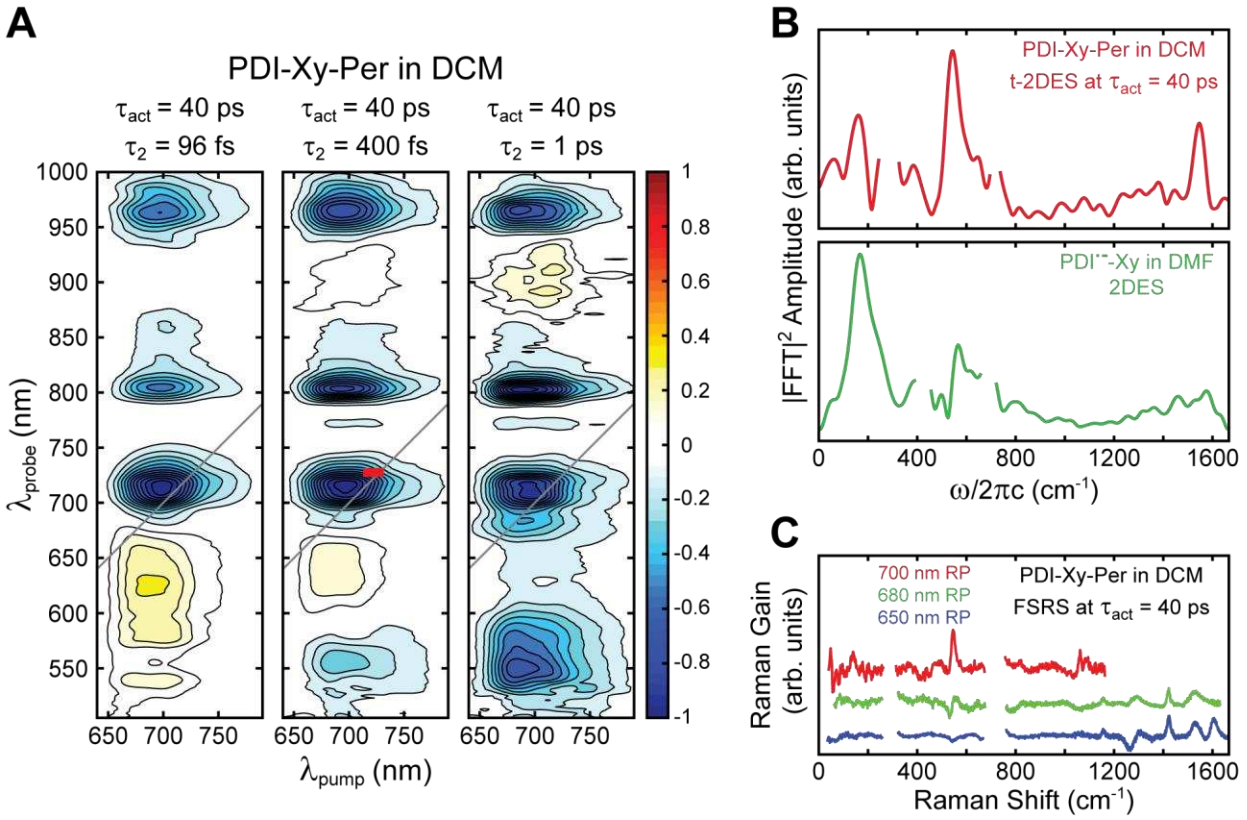

Figure 3. (A) t-2DES spectra of PDI-Xy-Per in DCM as a function of waiting time (τ_2), where the actinic pump delay (τ_{act}) is kept fixed at 40 ps. The spectra are normalized to the maximum absolute change in absorption at each (τ_{act}, τ_2). The red rectangle in center spectrum indicate the region over which coherence analysis has been performed. (B) Power spectra of coherent oscillations observed in t-2DES spectra of PDI-Xy-Per in DCM at τ_{act} = 40 ps (top) and in 2DES spectra of $PDI^{\bullet-}$-Xy in DMF (bottom). (C) FSRS spectra of PDI-Xy-Per in DCM at an actinic pump delay of 40 ps are shown for comparison.

160, 545, and 1550 cm^{-1}. In order to compare the coherent oscillations observed in the t-2DES spectra at τ_{act} = 40 ps, we performed a similar analysis on the conventional 2DES spectra of $PDI^{\bullet-}$-Xy in DMF (Figure 3B bottom panel). The three major $PDI^{\bullet-}$ centered vibrational modes appear here as expected. We also performed FSRS on PDI-Xy-Per in DCM with an actinic pump

at 525 nm, a Raman pump at 650, 680, and 700 nm, and a white-light probe pulse in order to further compare the vibrational coherences observed in t-2DES and 2DES experiments (Figure 3C). Even though the 160 cm^{-1} vibrational mode is not observed in FSRS due to insufficient spectral resolution in that region, such low frequency vibrational coherences have been previously

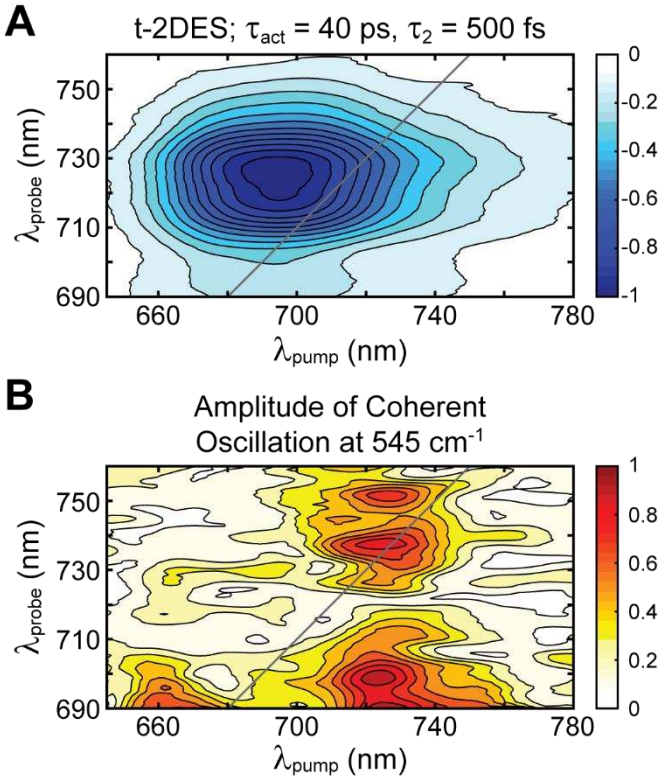

Figure 4. (A) t-2DES spectra of PDI-Xy-Per in DCM at ($\tau_{act,}$, τ_2) = 40 ps, 500 fs), showing the PIB signal around the diagonal. The spectrum is normalized to the maximum absolute change in absorption. (B) Normalized amplitude of the coherent oscillation at a frequency of 545 cm^{-1} obtained at each point of the t-2DES spectra shown in (A).

observed in 2DES studies of neutral PDI.[37, 41] The 545 and 1550 cm^{-1} vibrational coherence frequencies are assigned to $PDI^{\bullet-}$ centered modes using DFT calculations (see Figure S11), which are in good agreement with previous studies of PDI-Xy-Per.[36]

A comparison of coherent oscillations obtained from t-2DES spectra with FSRS spectra shows the dependence of resonance enhancement on electronic excitation wavelength and the importance of pump spectral resolution (Figures 3B and 3C). Since the vibrational coherences can be obtained

from each point in the t-2DES spectra, this technique can be instrumental in identifying the electronic excitation energies where vibrational resonance enhancements are maximized. To illustrate this feature of t-2DES, the intensity of the 545 cm^{-1} core stretch (Figure S11) vibrational mode obtained from the coherence analysis at different points of the PIB feature around 717 nm probe wavelength of t-2DES spectra at τ_{act} = 40 ps is shown in Figure 4B, along with the raw t-2DES spectra (Figure 4A). The two-dimensional contour map in Figure 4B shows that the resonance enhancement of this vibration is maximized at an excitation wavelength of 725 nm. Such excitation energy dependence of the resonance enhancement of vibrational intensities is the likely reason for the absence of the 1420 cm^{-1} mode in the power spectrum of the coherences obtained from t-2DES, which is present in the FSRS spectra at both 650 nm and 680 nm Raman pump wavelengths. These contour maps, often called beat maps, can provide useful constraints for detailed modeling of vibronic and/or electronic coupling of the system.[15, 42] The beat maps also highlight the relevant region of t-2DES spectra for coherence analysis, improving its signal-to-noise compared to pump-pump-probe spectroscopy. While a comparison of the FSRS spectra with the power spectrum of the coherent oscillations in t-2DES allows us to conclude that the coherences observed in t-2DES of this model system are likely purely vibrational in origin, the pattern of the beat map suggests that some vibronic coupling may also be present.[43]

In summary, we have demonstrated t-2DES on an electron donor-acceptor dyad molecule that undergoes photoinduced charge separation, measuring using 2DES at different stages of the charge transfer process. Moreover, we have shown that analysis of the amplitude oscillations of the t-2DES spectral features enables interrogation of vibrational coherences, and how they reflect changes in the potential energy surface(s) during a photophysical process. In this case, the 6.22 ps charge separation time constant is long enough that most coherences that can be measured in

conventional 2DES experiments have already dephased. The t-2DES experimental technique, therefore, can be employed to investigate the role of vibronic coupling on photoinduced electron transfer and other photophysical processes in chemical, biological, and materials systems through initiation and measurement of coherences at arbitrary positions along the reaction coordinate.

ASSOCIATED CONTENT

Supporting Information

The Supporting Information is available free of charge on the ACS Publications website at DOI:10.1021/acs.jpclett.XXXXX.

AUTHOR INFORMATION

Corresponding Author

Email: m-wasielewski@northwestern.edu

ryan.young@northwestern.edu

ORCID

Aritra Mandal: 0000-0002-8680-3730

Michael R. Wasielewski: 0000-0003-2920-5440

Ryan M. Young: 0000-0002-5108-0261

Notes

The authors declare no competing financial interest.

ACKNOWLEDGEMENTS

This work was supported by the National Science Foundation under grant no. DMR-1710104. J.D.S. gratefully acknowledges National Science Foundation Graduate Research Fellowship Program under Grant No. DGE-1842165. Any opinions, findings, and conclusions or recommendations expressed in this material are those of the author(s) and do not necessarily reflect the views of the National Science Foundation.

REFERENCES

1. Engel, G. S.; Calhoun, T. R.; Read, E. L.; Ahn, T.-K.; Mančal, T.; Cheng, Y.-C.; Blankenship, R. E.; Fleming, G. R., Evidence for Wavelike Energy Transfer through Quantum Coherence in Photosynthetic Systems. *Nature* **2007**, *446*, 782-786.

2. Scholes, G. D.; Fleming, G. R.; Chen, L. X.; Aspuru-Guzik, A.; Buchleitner, A.; Coker, D. F.; Engel, G. S.; Van Grondelle, R.; Ishizaki, A.; Jonas, D. M., Using Coherence to Enhance Function in Chemical and Biophysical Systems. *Nature* **2017**, *543*, 647-656.

3. Chenu, A.; Scholes, G. D., Coherence in Energy Transfer and Photosynthesis. *Annu. Rev. Phys. Chem.* **2015**, *66*, 69-96.

4. Collini, E.; Scholes, G. D., Coherent Intrachain Energy Migration in a Conjugated Polymer at Room Temperature. *Science* **2009**, *323*, 369-373.

5. Panitchayangkoon, G.; Hayes, D.; Fransted, K. A.; Caram, J. R.; Harel, E.; Wen, J.; Blankenship, R. E.; Engel, G. S., Long-Lived Quantum Coherence in Photosynthetic Complexes at Physiological Temperature. *Proc. Natl. Acad. Sci. USA* **2010**, *107*, 12766-12770.

6. Brixner, T.; Stenger, J.; Vaswani, H. M.; Cho, M.; Blankenship, R. E.; Fleming, G. R., Two-Dimensional Spectroscopy of Electronic Couplings in Photosynthesis. *Nature* **2005**, *434*, 625-628.

7. Calhoun, T. R.; Ginsberg, N. S.; Schlau-Cohen, G. S.; Cheng, Y.-C.; Ballottari, M.; Bassi, R.; Fleming, G. R., Quantum Coherence Enabled Determination of the Energy Landscape in Light-Harvesting Complex II. *J. Phys. Chem. B* **2009**, *113*, 16291-16295.

8. Ginsberg, N. S.; Cheng, Y.-C.; Fleming, G. R., Two-Dimensional Electronic Spectroscopy of Molecular Aggregates. *Acc. Chem. Res.* **2009**, *42*, 1352-1363.

9. Romero, E.; Augulis, R.; Novoderezhkin, V. I.; Ferretti, M.; Thieme, J.; Zigmantas, D.; Van Grondelle, R., Quantum Coherence in Photosynthesis for Efficient Solar-Energy Conversion. *Nat.*

Phys. **2014**, *10*, 676-682.

10. Tiwari, V.; Peters, W. K.; Jonas, D. M., Electronic Resonance with Anticorrelated Pigment Vibrations Drives Photosynthetic Energy Transfer Outside the Adiabatic Framework. *Proc. Natl. Acad. Sci. USA* **2013**, *110*, 1203-1208.

11. Fuller, F. D.; Pan, J.; Gelzinis, A.; Butkus, V.; Senlik, S. S.; Wilcox, D. E.; Yocum, C. F.; Valkunas, L.; Abramavicius, D.; Ogilvie, J. P., Vibronic Coherence in Oxygenic Photosynthesis. *Nat. Chem.* **2014**, *6*, 706-711.

12. Hwang, I.; Scholes, G. D., Electronic Energy Transfer and Quantum-Coherence in Π-Conjugated Polymers. *Chem. Mater.* **2010**, *23*, 610-620.

13. Halpin, A.; Johnson, P. J.; Tempelaar, R.; Murphy, R. S.; Knoester, J.; Jansen, T. L.; Miller, R. D., Two-Dimensional Spectroscopy of a Molecular Dimer Unveils the Effects of Vibronic Coupling on Exciton Coherences. *Nat. Chem.* **2014**, *6*, 196-201.

14. Hayes, D.; Griffin, G. B.; Engel, G. S., Engineering Coherence among Excited States in Synthetic Heterodimer Systems. *Science* **2013**, *340*, 1431-1434.

15. Bakulin, A. A.; Morgan, S. E.; Kehoe, T. B.; Wilson, M. W.; Chin, A. W.; Zigmantas, D.; Egorova, D.; Rao, A., Real-Time Observation of Multiexcitonic States in Ultrafast Singlet Fission Using Coherent 2D Electronic Spectroscopy. *Nat. Chem.* **2016**, *8*, 16-23.

16. Hybl, J. D.; Albrecht, A. W.; Faeder, S. M. G.; Jonas, D. M., Two-Dimensional Electronic Spectroscopy. *Chem. Phys. Lett.* **1998**, *297*, 307-313.

17. Cho, M., Coherent Two-Dimensional Optical Spectroscopy. *Chem. Rev.* **2008**, *108*, 1331-1418.

18. Rafiq, S.; Scholes, G. D., From Fundamental Theories to Quantum Coherences in Electron Transfer. *J. Am. Chem. Soc.* **2019**, *141*, 708-722.

19. Policht, V. R.; Niedringhaus, A.; Ogilvie, J. P., Characterization of Vibrational Coherence in Monomeric Bacteriochlorophyll a by Two-Dimensional Electronic Spectroscopy. *J. Phys. Chem. Lett.* **2018**, *9*, 6631-6637.

20. Musser, A. J.; Liebel, M.; Schnedermann, C.; Wende, T.; Kehoe, T. B.; Rao, A.; Kukura, P., Evidence for Conical Intersection Dynamics Mediating Ultrafast Singlet Exciton Fission. *Nat. Phys.* **2015**, *11*, 352-357.

21. Mandal, A.; Chen, M.; Foszcz, E. D.; Schultz, J. D.; Kearns, N. M.; Young, R. M.; Zanni, M. T.; Wasielewski, M. R., Two-Dimensional Electronic Spectroscopy Reveals Excitation Energy-Dependent State Mixing During Singlet Fission in a Terrylenediimide Dimer. *J. Am. Chem. Soc.* **2018**, *140*, 17907-17914.

22. Auböck, G.; Consani, C.; van Mourik, F.; Chergui, M., Ultrabroadband Femtosecond Two-Dimensional Ultraviolet Transient Absorption. *Opt. Lett.* **2012**, *37*, 2337-2339.

23. Bredenbeck, J.; Helbing, J.; Hamm, P., Labeling Vibrations by Light: Ultrafast Transient 2D-IR Spectroscopy Tracks Vibrational Modes During Photoinduced Charge Transfer. *J. Am. Chem. Soc.* **2004**, *126*, 990-991.

24. Xiong, W.; Laaser, J. E.; Paoprasert, P.; Franking, R. A.; Hamers, R. J.; Gopalan, P.; Zanni, M. T., Transient 2D IR Spectroscopy of Charge Injection in Dye-Sensitized Nanocrystalline Thin Films. *J. Am. Chem. Soc.* **2009**, *131*, 18040-18041.

25. Hunt, N., Transient 2D-IR Spectroscopy of Inorganic Excited States. *Dalton Trans.* **2014**, *43*, 17578-17589.

26. Frontiera, R. R.; Mathies, R. A., Femtosecond Stimulated Raman Spectroscopy. *Laser & Photonics Reviews* **2011**, *5*, 102-113.

27. Kukura, P.; McCamant, D. W.; Mathies, R. A., Femtosecond Stimulated Raman Spectroscopy.

Annu. Rev. Phys. Chem. **2007**, *58*, 461-488.

28. Hauer, J.; Buckup, T.; Motzkus, M., Pump-Degenerate Four Wave Mixing as a Technique for Analyzing Structural and Electronic Evolution: Multidimensional Time-Resolved Dynamics near a Conical Intersection. *J. Phys. Chem. A* **2007**, *111*, 10517-10529.

29. Molesky, B. P.; Guo, Z.; Cheshire, T. P.; Moran, A. M., Perspective: Two-Dimensional Resonance Raman Spectroscopy. *J. Chem. Phys.* **2016**, *145*, 180901.

30. Wende, T.; Liebel, M.; Schnedermann, C.; Pethick, R. J.; Kukura, P., Population-Controlled Impulsive Vibrational Spectroscopy: Background-and Baseline-Free Raman Spectroscopy of Excited Electronic States. *J. Phys. Chem. A* **2014**, *118*, 9976-9984.

31. Kraack, J. P.; Wand, A.; Buckup, T.; Motzkus, M.; Ruhman, S., Mapping Multidimensional Excited State Dynamics Using Pump-Impulsive-Vibrational-Spectroscopy and Pump-Degenerate-Four-Wave-Mixing. *Phys. Chem. Chem. Phys.* **2013**, *15*, 14487-14501.

32. Liebel, M.; Kukura, P., Broad-Band Impulsive Vibrational Spectroscopy of Excited Electronic States in the Time Domain. *J. Phys. Chem. Lett.* **2013**, *4*, 1358-1364.

33. Roeding, S.; Brixner, T., Coherent Two-Dimensional Electronic Mass Spectrometry. *Nat. Commun.* **2018**, *9*, 2519.

34. Ruetzel, S.; Kullmann, M.; Buback, J.; Nuernberger, P.; Brixner, T., Tracing the Steps of Photoinduced Chemical Reactions in Organic Molecules by Coherent Two-Dimensional Electronic Spectroscopy Using Triggered Exchange. *Phys. Rev. Lett.* **2013**, *110*, 148305.

35. Spencer, A. P.; Hutson, W. O.; Harel, E., Quantum Coherence Selective 2D Raman–2D Electronic Spectroscopy. *Nat. Commun.* **2017**, *8*, 14732.

36. Brown, K. E.; Veldkamp, B. S.; Co, D. T.; Wasielewski, M. R., Vibrational Dynamics of a Perylene–Perylenediimide Donor–Acceptor Dyad Probed with Femtosecond Stimulated Raman

Spectroscopy. *J. Phys. Chem. Lett.* **2012**, *3*, 2362-2366.

37. Tekavec, P. F.; Myers, J. A.; Lewis, K. L.; Ogilvie, J. P., Two-Dimensional Electronic Spectroscopy with a Continuum Probe. *Opt. Lett.* **2009**, *34*, 1390-1392.

38. Grumstrup, E. M.; Shim, S.-H.; Montgomery, M. A.; Damrauer, N. H.; Zanni, M. T., Facile Collection of Two-Dimensional Electronic Spectra Using Femtosecond Pulse-Shaping Technology. *Optics Express* **2007**, *15*, 16681-16689.

39. Ding, F.; Fulmer, E. C.; Zanni, M. T., Heterodyned Fifth-Order Two-Dimensional IR Spectroscopy: Third-Quantum States and Polarization Selectivity. *J. Chem. Phys.* **2005**, *123*, 094502.

40. Brown, K. E.; Salamant, W. A.; Shoer, L. E.; Young, R. M.; Wasielewski, M. R., Direct Observation of Ultrafast Excimer Formation in Covalent Perylenediimide Dimers Using near-Infrared Transient Absorption Spectroscopy. *J. Phys. Chem. Lett.* **2014**, *5*, 2588-2593.

41. Mančal, T.; Bixner, O.; Christensson, N.; Hauer, J.; Milota, F.; Nemeth, A.; Sperling, J.; Kauffmann, H. F., Dynamics of Quantum Wave Packets in Complex Molecules Traced by 2D Coherent Electronic Correlation Spectroscopy. *Procedia Chem.* **2011**, *3*, 105-117.

42. Dean, J. C.; Rafiq, S.; Oblinsky, D. G.; Cassette, E.; Jumper, C. C.; Scholes, G. D., Broadband Transient Absorption and Two-Dimensional Electronic Spectroscopy of Methylene Blue. *J. Phys. Chem. A* **2015**, *119*, 9098-9108.

43. Butkus, V.; Zigmantas, D.; Valkunas, L.; Abramavicius, D., Vibrational vs. Electronic Coherences in 2D Spectrum of Molecular Systems. *Chem. Phys. Lett.* **2012**, *545*, 40-43.